INTERNATIONAL JOURNAL OF ADVANCE RESEARCH, IDEAS AND INNOVATIONS IN TECHNOLOGY

ISSN: 2454-132X
Impact Factor: 6.078
(Volume 12, Issue 6 - V12I6-1156)
Available online at: https://www.ijariit.com

Thermal Performance Enhancement of Battery Systems using Porous Media with Optimized Layer Distribution

Arun Ramachandran
rarunmech11@gmail.com
Brandenburg Technical University, Cottbus, Germany

Sree Vidya T R
trsreevidya@tagore-engg.ac.in
Tagore Engineering College, Rathinamangalam, Tamil Nadu

ABSTRACT

Lithium-ion batteries generate heat during high-rate operation, and inadequate heat removal can accelerate degradation and increase safety risks. This study numerically investigates forced-air cooling of cylindrical lithium-ion cells with porous aluminium media distributed around the cell surface. Configurations with no porous media and with 3, 5, and 7 porous layers are compared, followed by an assessment of asymmetric layer arrangements in a three-cell inline system. The reported single-cell maximum temperature decreases from approximately 31.86 °C without porous media to 30.76 °C, 30.37 °C, and 30.05 °C for the 3-, 5-, and 7-layer cases, respectively. In the multi-cell study, downstream cells experience higher temperatures because the cooling air warms along the flow direction. The study identifies a non-uniform layer distribution as a promising design approach: fewer layers can be used near the inlet, while additional layers can be assigned to downstream cells. Porous media increases the reported pressure drop by approximately 40% relative to the baseline, so thermal benefits must be assessed alongside flow resistance. These results indicate that porous aluminium combined with forced air can improve battery temperature control, while layer-wise optimization may balance cooling performance and structural complexity.

Keywords: *Battery Thermal Management, Lithium-Ion Battery, Porous Aluminium, Forced-Air Cooling, Thermal*

1. INTRODUCTION

Lithium-ion batteries are widely used in electric vehicles, aircraft systems, and energy-storage applications because of their high energy density and power capability. During charging and discharging, internal resistance and electrochemical processes generate heat. If this heat is not removed effectively, cell temperature can rise, accelerating capacity degradation and reducing service life. In severe cases, elevated temperature can contribute to thermal runaway and propagation between cells.

In aircraft, lithium-ion batteries are considered for more-electric aircraft systems, auxiliary power, and electric or hybrid-electric propulsion concepts, including emerging electric vertical take-off and landing (eVTOL) platforms. Their high specific energy and power capability can help reduce dependence on conventional energy sources, but aircraft applications place strong emphasis on low mass, compact packaging, reliability, and safe operation. High-power take-off, climb, and other peak-load conditions can produce substantial heat within the cells; therefore, battery thermal management must limit peak temperature and cell-to-cell temperature differences without imposing excessive mass or airflow pressure loss. The present study examines porous-media-assisted forced-air cooling at the cell level; it does not model a complete aircraft battery pack or validate an aircraft installation.

Battery thermal management systems (BTMS) use air cooling, liquid cooling, phase-change materials, heat pipes, or combinations of these approaches. Air cooling is relatively simple, but its effectiveness can be limited by the available heat-transfer area and by warming of the air as it passes through a battery pack. Porous metal structures can increase the effective surface area and promote mixing, potentially improving convective heat transfer. Their use also introduces flow resistance and pressure drop, which must be considered in the design.

This work evaluates porous aluminium layers around cylindrical cells under forced-air cooling. The main objectives are to compare 3-, 5-, and 7-layer configurations, examine temperature variation across three inline cells, and assess whether an asymmetric layer distribution can provide a useful balance between thermal performance and pressure loss.

© 2026, IJARIIT - All rights reserved.

2. COMPUTATIONAL METHODOLOGY

2.1 Geometry and computational domain

The study models cylindrical lithium-ion cells arranged in an aligned configuration. The cell dimensions reported in the project are approximately 18.24 mm in diameter and 65.1 mm in height. The three-cell arrangement is positioned along the airflow direction so that inlet, middle, and downstream thermal behavior can be compared. The computational domain includes an entrance region, a main region containing the cells, and an extended outlet region to reduce the influence of boundary effects on the flow field. The porous aluminum structure is represented as a homogeneous porous region rather than resolving individual pores. The project describes a porous region with a nominal thickness of 5 mm and porosity of 0.958. Configurations with 3, 5, and 7 discrete layers are compared. The reported axial spacing between layers is 13 mm, 9 mm, and 5 mm for the 3-, 5-, and 7-layer arrangements, respectively.

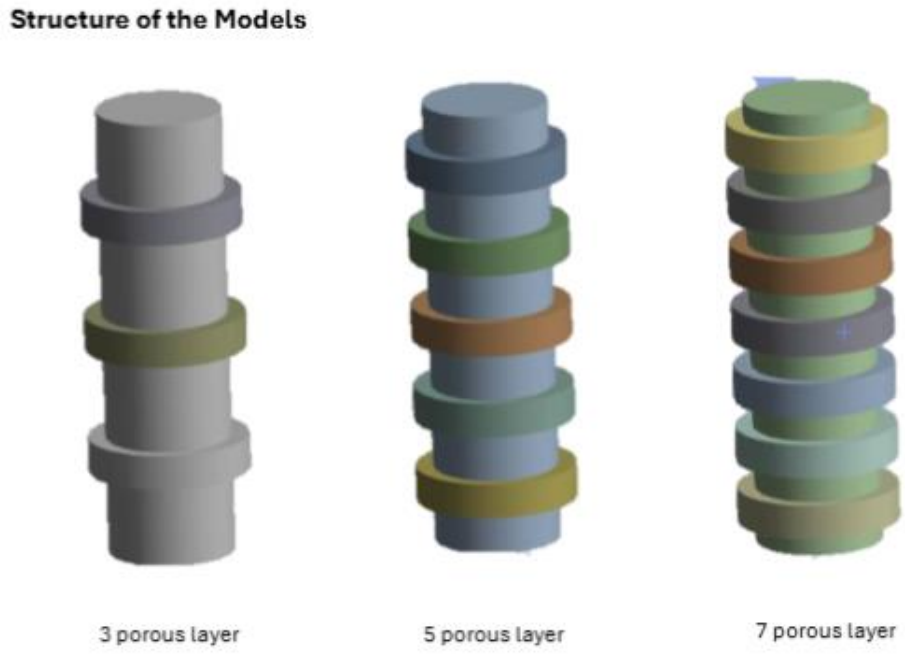


Figure-1: Source model configurations with 3, 5, and 7 porous layers

2.2 LTE and LTNE modelling in porous media

Local thermal equilibrium (LTE) assumes that the porous solid matrix and cooling air have the same local temperature, so a single energy equation can represent the combined medium. This approximation is most suitable when solid–fluid interfacial heat transfer is sufficiently strong. Local thermal non-equilibrium (LTNE) permits separate solid and fluid temperatures and is more appropriate when the phases respond at different rates, for example under high heat flux or limited interfacial exchange. The source project describes a homogeneous porous-zone Darcy–Forchheimer treatment; it does not clearly document a separately solved LTNE model. LTE/LTNE equations below are therefore presented as modelling options, not as a claim that both were implemented in the original simulation.

LTE energy model: $(\rho c_p)_{eff}\,\partial T/\partial t + \nabla\cdot(\rho\, c_p\, u\cdot\nabla T) = \nabla\cdot(k_{eff}\nabla T) + q'''$

LTNE solid phase: $(1-\varepsilon)\rho_s\, c_{ps}\,\partial T_s/\partial t = \nabla\cdot(k_s\,\nabla T_s) + h_{sf}\, a_s\,(Tf-Ts)$

LTNE fluid phase: $\varepsilon\rho_f\, c_{pf}\partial T_f/\partial t + \varepsilon\rho f\, c_{pf}\, u\cdot\nabla Tf = \nabla\cdot(k_f\nabla T_f) + h_{sf}\, a_s\,(T_s-T_f)$

where $(\rho c_p)_{eff}$ and (k_{eff} represent the effective heat capacity and thermal conductivity of the porous medium. The LTE model is computationally efficient and widely used in preliminary simulations. However, in practical BTMS applications, especially under high heat generation rates and forced convection, the temperature difference between solid and fluid phases becomes significant. In such cases, the LTNE model provides a more accurate representation by solving two separate energy equations

Where ε represents the porosity of the material, h_{sf} denotes the interfacial heat transfer coefficient between the solid and fluid phases, and \(a_s\) refers to the specific surface area. The Local Thermal Non-Equilibrium (LTNE) model accounts for the temperature difference between the solid and fluid phases, making it suitable for analyzing heat transfer in metal foams, highly porous materials, and battery thermal management systems subjected to non-uniform heating.

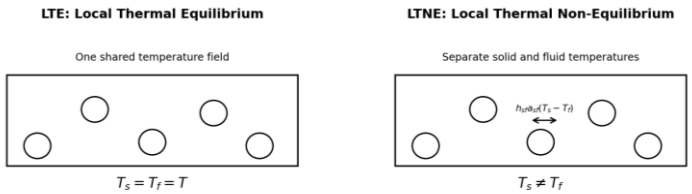


Figure-2: comparison of LTE and LTNE porous-medium thermal models

2.3 Material properties and flow model

Air is used as the cooling fluid, with properties specified at 300 K. The porous medium is aluminium foam represented using a Darcy–Forchheimer resistance model in ANSYS Fluent. This continuum approach incorporates viscous and inertial pressure losses without explicitly resolving the internal pore geometry.

Table-1: Air properties at 30o C

Parameters		Value	Unit
Density (ρ)		1.164	kg/m³
Dynamic viscosity (μ)		1.85×10^{-5}	Pa·s
Specific heat at constant pressure (Cp)		1005	J/(kg·K)
Thermal conductivity ()k		0.0263	W/(m·K)
Prandtl number(Pr)		0.707	—

Table-2: Air properties of Porous media Aluminum

Porous-medium parameter	Value	Unit
Permeability K	1.42×10^{-6}	m²
Inertial coefficient C_t	0.340	—
Porosity ε	0.958	—
Pore diameter d_f	8×10^{-4}	m
Viscous resistance 1/K	7.04×10^{5}	m^{-2}

Table-3: Properties of the 18650 Li-ion Battery Implemented in This Study

Li-ion parameter	*Value*	*Unit*
Normal capacity	*3200*	*mAh*
Nominal Voltage	*3.56*	*V*
Maximum Discharge Current	*6400*	*mA*
Density (ρ)	*2092*	*kg/m³*
Specific Heat Capacity (Cp)	*678*	*J/(kg·K)*
Specific Heat Capacity (k_x, k_y)	*18.25*	*W/(m·K)*
Thermal Conductivity (kz)	*1*	*W/(m·K)*
Internal Resistance (Ri)	*29*	*mΩ*

2.4 Battery heat generation

Battery heat generation is applied as a volumetric heat source. The project specifies a heat-source value of 70,000 W/m³ to represent operation at a high load corresponding to a 2C discharge rate. The battery material is treated as homogeneous and isotropic for the thermal simulation, with constant thermophysical properties. These assumptions simplify the computational model and support comparison of the porous-layer configurations.

For a volumetric source, the total heat input is $\dot{Q} = q''' V_{cell}$. If a current/resistance-based estimate is available, irreversible heating may be approximated as $\dot{Q}_{irr} = I^2R$; a more complete electrochemical expression can include reversible entropic heating. The source project specifies q‴ = 70,000 W/m³, but does not provide enough information here to independently derive that value from current and resistance.

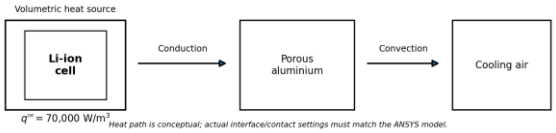


Figure-3: Heat-generation and heat-removal path in the battery thermal management system

2.5 Configurations evaluated

The study first compares a single cell without porous media and with 3, 5, and 7 layers. It then examines three inline cells to evaluate the effect of airflow direction. Three asymmetric arrangements are reported: Model 1 (3–5–7), Model 2 (3–3–5 in the arrangement table), and Model 3 (3–7–5 in the arrangement table). The project's conclusion separately identifies a 3–3–7 arrangement as the preferred configuration; this inconsistency in the original model labels should be reconciled against the simulation files before publication.

2.6 Boundary conditions and governing equations

The computational domain uses a velocity inlet for the incoming cooling air and a pressure outlet downstream. The outer domain boundaries are treated as walls where indicated by the model geometry; the cylindrical cell surface is a no-slip wall for the air and a heat-transfer interface with the generated cell heat. The porous aluminium is modelled as a porous zone using Darcy–Forchheimer momentum resistance.

$$\text{Continuity: } \nabla \cdot (\rho u) = 0$$

Heat source used in the project: q‴ = 70,000 W/m³. The reported cell maximum temperature is compared across the baseline and 3-, 5-, and 7-layer cases.

3. RESULT AND DISCUSSION

3.1 Single-cell temperature response

The reported temperature contours show a consistent decrease in maximum cell temperature as the number of porous layers increases. The baseline case has a maximum temperature of approximately 31.86 °C. Adding three layers reduces this value to 30.76 °C, while five layers reduce it to 30.37 °C. The seven-layer configuration reaches approximately 30.05 °C and provides the lowest peak temperature among the tested single-cell cases.

Table-4: Reduction from baseline temperature for 3, 5 and 7 layer

Configuration	Maximum temperature °C	Reduction from baseline °C
No porous media	31.86	0.00
3 layers	30.76	1.10
5 layers	30.37	1.49
7 layers	30.05	1.81

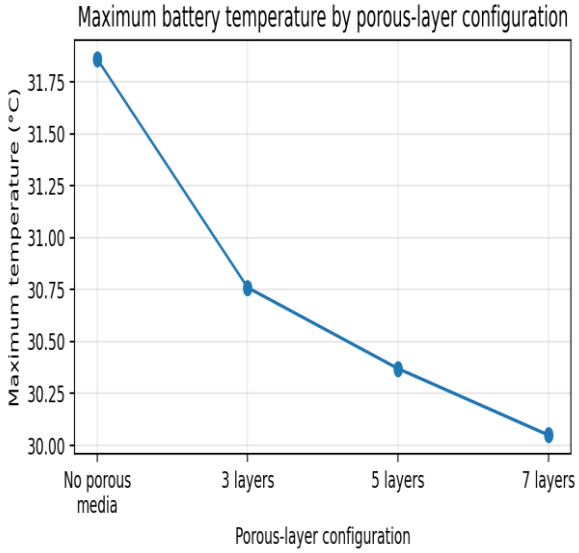


Figure-4: Maximum temperature Vs Porous layer configuaration

Interpretation: the plotted values are maximum cell temperatures reported by the source project; the reduction is calculated relative to the 31.86 °C baseline. These are model outputs, not experimental measurements.

Compared with the baseline, the 7-layer configuration reduces the reported maximum temperature by about 1.81 °C. The close spacing of the layers is associated in the project with more continuous thermal coverage and improved temperature uniformity. The result suggests that increasing layer count improves cooling for the modeled conditions, although added layers increase design complexity and may raise flow resistance.

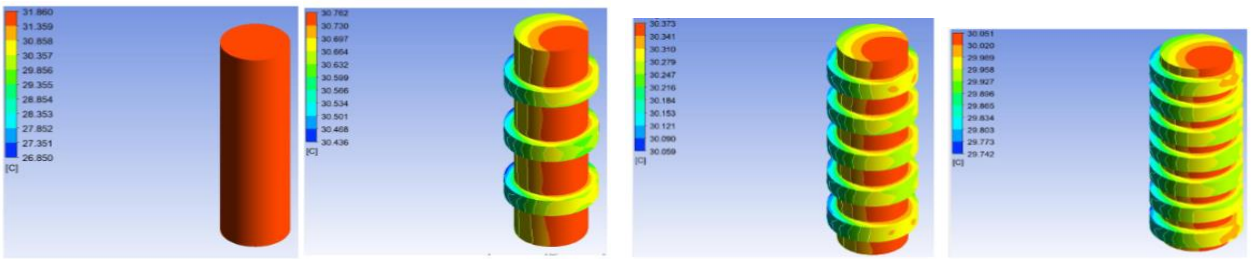


Figure-5: Temperature distribution for No layer, 3, 5, 7 layer in Cell

3.2 Temperature distribution in cells

The multi-cell contours show that the first cell near the inlet is generally cooler than downstream cells. As air passes over each cell, it absorbs heat and becomes warmer, reducing its ability to remove heat from cells farther downstream. This produces a position-dependent temperature gradient even when the cells have similar geometry and heat generation.

Porous layers improve heat removal at all three positions, but the cooling benefit depends on the local airflow temperature and the layer distribution. The reported temperature-reduction table is reproduced below. The values should be checked against the final simulation exports because the arrangement names and layer counts differ in places within the source project.

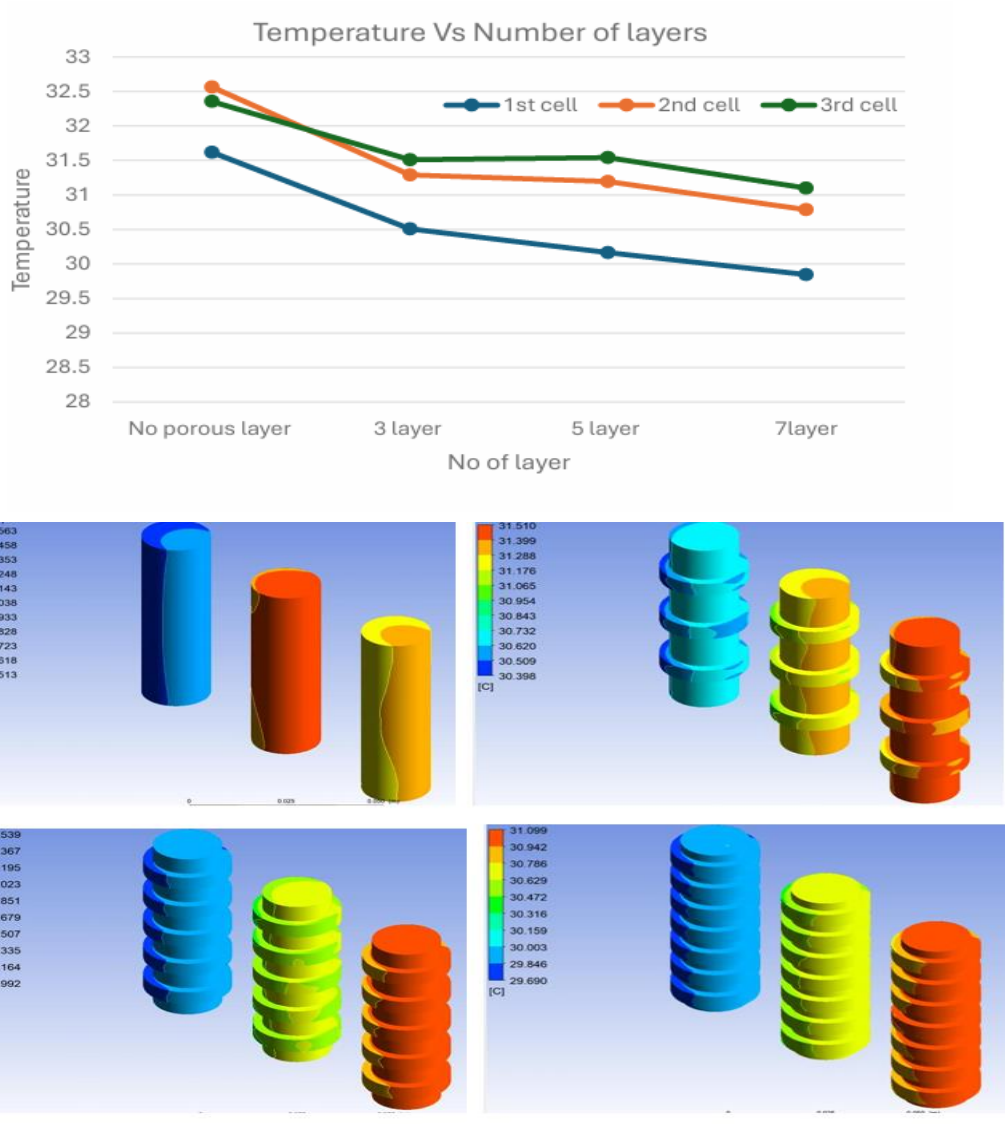


Figure-6: Temperature-versus-number-of-layers plot and corresponding temperature plot

Table-5: Temperature Reduction Model 1, Model 2 and Model 3

Reported model	1st cell reduction (°C)	2nd cell reduction (°C)	3rd cell reduction (°C)
Model 1 (3–5–7)	1.004	1.621	0.972
Model 2 (3–3–7)	1.038	1.252	1.408
Model 3 (3–7–7)	1.015	1.643	1.011

3.3 Pressure-drop comparison

The baseline configuration without porous media has a reported pressure drop of 4.285 Pa. With porous media, Model 1 has a pressure drop of 6.002 Pa, Model 2 has 6.007 Pa, and Model 3 has 5.958 Pa. The corresponding increases are 1.717 Pa, 1.722 Pa, and 1.673 Pa, respectively. These values represent increases of approximately 40% relative to the baseline.

Table-6: Pressure drop across Model 1, Model 2 and Model 3

Configuration	Pressure drop (Pa)	Increase over baseline (Pa)	Approx. increase (%)
No porous media	4.285	—	—
Model 1	6.002	1.717	40.1
Model 2	6.007	1.722	40.2
Model 3	5.958	1.673	39.0

The pressure-drop results indicate that the presence of porous media is the main contributor to the increase in flow resistance. The difference between Model 1 and Model 2 is only 0.005 Pa, which is negligible relative to their total pressure drops. Consequently, the design decision should consider both temperature reduction and the fan or blower power required to overcome the added resistance.

4. DESIGN IMPLICATIONS

The results support a layer-wise design strategy rather than assuming that every cell requires the same porous-layer count. Fresh inlet air provides stronger cooling to the upstream cell, whereas downstream cells encounter warmer air and may need additional thermal enhancement. An asymmetric configuration could therefore place fewer layers near the inlet and more layers downstream, potentially reducing unnecessary material while improving temperature uniformity. However, the preferred arrangement must be established using consistent model labels and direct comparisons of maximum temperature, cell-to-cell temperature difference, and pressure drop.

The reported simulations are numerical and depend on the assumed heat generation, air properties, porous resistance coefficients, and boundary conditions. Before publication, the mesh-independence procedure, inlet velocity, turbulence model, thermal boundary conditions, convergence criteria, and uncertainty or validation evidence should be documented. The current project text does not provide enough complete information to independently reproduce these items.

5. CONCLUSION

This numerical study evaluates porous aluminium media as a heat-transfer enhancement method for forced-air cooling of lithium-ion battery cells. For the single-cell model, the maximum temperature decreases from approximately 31.86 °C without porous media to 30.05 °C with seven layers. The 3-layer and 5-layer cases reach 30.76 °C and 30.37 °C, respectively. The trend indicates improved thermal performance as layer count increases under the modeled conditions.

In the inline-cell model, downstream cells are exposed to warmer air and tend to experience higher temperatures, demonstrating the importance of airflow direction in multi-cell battery thermal management. Porous media reduces temperature rise but increases pressure drop from 4.285 Pa in the baseline to approximately 5.958–6.007 Pa in the porous cases. This is an approximately 39–40% increase in pressure drop.

A non-uniform porous-layer arrangement is a promising design direction because it can allocate more cooling structure to downstream cells. Nevertheless, the source project contains inconsistencies between the layer arrangements in the model table, the temperature-reduction table, and the stated preferred 3–3–7 configuration. Those labels and the underlying numerical results should be verified before submission. Further work should report complete boundary conditions, mesh independence, validation, and fan-power implications to strengthen the publication.

REFERENCES

[1] R. Alhindawi, Y. Abu Nahleh, A. Kumar, and N. Shiwakoti, “Projection of Greenhouse Gas Emissions for the Road Transport Sector Based on Multivariate Regression and the Double Exponential Smoothing Model,” *Sustainability*, vol. 12, 2020.

[2] A. Pesaran, M. Keyser, G. H. Kim, S. Santhanagopalan, and K. Smith, “Tools for Designing Thermal Management of Batteries in Electric Drive Vehicles (Presentation),” United States, 2013.

[3] A. A. Pesaran, “Battery thermal models for hybrid vehicle simulations,” *Journal of Power Sources*, vol. 110, pp. 377–382, 2002.

[4] A. Börger, J. Mertens, and H. Wenzl, “Thermal runaway and thermal runaway propagation in batteries: What do we talk about?” *Journal of Energy Storage*, vol. 24, Article 100649, 2019.

[5] X. Feng, M. Ouyang, X. Liu, L. Lu, Y. Xia, and X. He, “Thermal runaway mechanism of lithium ion battery for electric vehicles: A review,” *Energy Storage Materials*, vol. 10, pp. 246–267, 2018.

[6] M. J. Loveridge, G. Remy, N. Kourra, R. Genieser, A. Barai, M. J. Lain, et al., “Looking Deeper into the Galaxy (Note 7),” *Batteries*, vol. 4, 2018.

[7] L. Li, X. Ju, X. Zhou, Y. Peng, Z. Zhou, B. Cao, et al., “Experimental study on thermal runaway process of 18650 lithium-ion battery under different discharge currents,” *Materials*, vol. 14, 2021.

[8] H. Chen, J. E. H. Buston, J. Gill, D. Howard, R. C. E. Williams, C. M. Rao Vendra, et al., “An experimental study on thermal runaway characteristics of lithium-ion batteries with high specific energy and prediction of heat release rate,” *Journal of Power Sources*, vol. 472, Article 228585, 2020.

[9] P. R. Tete, M. M. Gupta, and S. S. Joshi, “Developments in battery thermal management systems for electric vehicles: A technical review,” *Journal of Energy Storage*, vol. 35, Article 102255, 2021.

[10] F. Zhang, A. Lin, P. Wang, and P. Liu, “Optimization design of a parallel air-cooled battery thermal management system with spoilers,” *Applied Thermal Engineering*, vol. 182, Article 116062, 2021.

[11] J. Zhang, X. Wu, K. Chen, D. Zhou, and M. Song, “Experimental and numerical studies on an efficient transient heat transfer model for air-cooled battery thermal management systems,” *Journal of Power Sources*, vol. 490, Article 229539, 2021.

[12] K. Chen, J. Hou, X. Wu, Y. Chen, M. Song, and S. Wang, “Design of flow pattern in air-cooled battery thermal management system,” *International Journal of Energy Research*, vol. 45, pp. 9541–9554, 2021.

[13] X. Li, J. Zhao, J. Duan, S. Panchal, J. Yuan, R. Fraser, et al., “Simulation of cooling plate effect on a battery module with different channel arrangement,” *Journal of Energy Storage*, vol. 49, Article 104113, 2022.

[14] X. Li, J. Zhao, J. Yuan, J. Duan, C. Liang, et al., “Simulation and analysis of air cooling configurations for a lithium-ion battery pack,” *Journal of Energy Storage*, vol. 35, Article 102270, 2021.

[15] M. Wang, T.-C. Hung, H. Xi, et al., “Numerical study on performance enhancement of the air-cooled battery thermal management system by adding parallel plates,” *Energies*, vol. 14, 2021.

[16] W. Yang, F. Zhou, H. Zhou, et al., "Thermal performance of axial air cooling system with bionic surface structure for cylindrical lithium-ion battery module," *International Journal of Heat and Mass Transfer*, vol. 161, Article 120307, 2020.

[17] K. Yu, X. Yang, Y. Cheng, and C. Li, "Thermal analysis and two-directional air flow thermal management for lithium-ion battery pack," *Journal of Power Sources*, vol. 270, pp. 193–200, 2014.

[18] S. Shahid and M. Agelin-Chaab, "Development and analysis of a technique to improve air-cooling and temperature uniformity in a battery pack for cylindrical batteries," *Thermal Science and Engineering Progress*, vol. 5, pp. 351–363, 2018.

[19] E. J., M. Yue, J. Chen, H. Zhu, Y. Deng, Y. Zhu, et al., "Effects of the different air cooling strategies on cooling performance of a lithium-ion battery module with baffle," *Applied Thermal Engineering*, vol. 144, pp. 231–241, 2018.

[20] J. Xie, Z. Ge, M. Zang, and S. Wang, "Structural optimization of lithium-ion battery pack with forced air cooling system," *Applied Thermal Engineering*, vol. 126, pp. 583–593, 2017.

[21] N. Yang, X. Zhang, G. Li, and D. Hua, "Assessment of the forced air-cooling performance for cylindrical lithium-ion battery packs: A comparative analysis between aligned and staggered cell arrangements," *Applied Thermal Engineering*, vol. 80, pp. 55–65, 2015.

[22] K. Egab and S. K. Oudah, "Thermal management analysis of Li-ion battery-based cooling system using dimples with air fins and perforated fins," *International Journal of Thermal Sciences*, vol. 171, Article 107200, 2022.

[23] H. Behi, D. Karimi, J. Jaguemont, F. H. Gandoman, T. Kalogiannis, and M. Berecibar, et al., "Novel thermal management methods to improve the performance of the Li-ion batteries in high discharge current applications," *Energy*, vol. 224, Article 120165, 2021.

[24] H. Behi, T. Kalogiannis, M. Suresh Patil, J. V. Mierlo, and M. Berecibar, "A new concept of air cooling and heat pipe for electric vehicles in fast discharging," *Energies*, vol. 14, 2021.

[25] L. H. Saw, Y. Ye, M. C. Yew, W. T. Chong, M. K. Yew, and T. C. Ng, "Computational fluid dynamics simulation on open cell aluminium foams for Li-ion battery cooling system," *Applied Energy*, vol. 204, pp. 1489–1499, 2017.